Eur. Phys. J. D **19**, 3–8 (2002)
DOI: 10.1140/epjd/e20020048

THE EUROPEAN PHYSICAL JOURNAL D
EDP Sciences

Excitation of hydrogen atom by positron using Hylleraas time-dependent approach

D.O. Odero[a]

Medical Physics, Division of Radiation Oncology, The Johns Hopkins University School of Medicine, Baltimore, Maryland 21231, USA

Received 23 July 2001 and Received in final form 25 November 2001

Abstract. The time-dependent treatment of positron-hydrogen scattering for a zero total angular momentum has been presented. The initial wavefunction of the positron-hydrogen scattering system has been expanded in terms of three dimensional dynamical wave functions to include all higher angular momenta by solving a set of three coupled differential equations. This wavefunction is then time evolved using Taylor series expansion of the evolution operator. The excitation probabilities are monitored as the wavefunction propagates until there is no more change in the probabilities. The positron impact excitation cross-sections extracted from the final wavefunction are compared with the available results of converged close coupling approach.

PACS. 34.80.-i Electron scattering – 34.85.+x Positron scattering – 36.10.Dr Positronium, muonium, muonic atoms and molecules

1 Introduction

Positron-hydrogen scattering system has three simplest and well defined charged particles, namely; electron, positron and proton. The simplistic nature of this scattering system is very attractive in the implementation of new theoretical methods. There has also been a growing interest in understanding the details of the origin of 511-keV annihilation radiation, which has been observed to be coming from the center of Milky Way galaxy and from solar flares [1,2]. Another interesting study involving this scattering system is on the creation of antihydrogen atoms resulting from positron transfer from the positronium to antiprotons [3].

Many theoretical treatments used in this field has been based on the solution of the time-independent Schrödinger equation [4–8]. Unfortunately, there has been disagreement in the results obtained within the intermediate energy range from these different approaches. Most of these methods do not include the positronium channels in the wavefunctions thus neglect the positronium contributions. This exclusion does not affect the results in the low and high energy regions where the positronium channels are not important [8–11]. Resonance have been observed from the multi-channel close coupling calculations, which should be reliable in the intermediate energy range [12–18]. The calculations based on the hyperspherical close coupling method [19] contradicted the existence of those resonances. The use of an over complete basis set and the possibility of double counting [20] is the major drawback with close coupling methods, which expand in terms of wavefunctions centered on both the proton and positron. However, when the positronium states are not included to avoid this double counting, the expansion becomes unreliable near the positronium formation threshold.

The most recent calculations in this field was based on the time-dependent close coupling (TDCC) approach [20]. However, this method exhibits slow convergence of the number of individual angular momentum (ℓ_1, ℓ_2) pairs, which are summed over for each total angular momentum L. The results from TDCC are very sensitive to the number of these pairs. Therefore, a significant number of these pairs are required for each L, which is not possible due to the computational limitation. Another time-dependent approach similar to TDCC but uses the Chebychev propagation scheme and Fast Fourier Transform to compute the integrals has also been developed and applied [21] to the S-wave model of Tempkin-Poet. This method would require large-scale calculation of partial waves, which are needed in the scattering flux for the real atomic system, a problem already noticed with TDCC [20]. Therefore, a method, which would automatically include all the scattering channels would be desirable.

Positron-hydrogen scattering process is inherently a time-dependent process. Thus a time-dependent treatment is attractive. An approach that involves a direct integration of the time-dependent Schrödinger equation

[a] *Present address:* St. Francis Center, 1700 SW 7th St, Topeka, KS 66606-1690, USA.
e-mail: dodero@msm.umr.edu

(referred to as the time-dependent Hylleraas (TDH)) method has been developed [22–28]. In this method, the system wavefunction is expanded in terms of three dynamical variables (two radial and one angular components) and then time evolved from the initial known state. This approach is reliable for all energy ranges and represents an attractive alternative approach for the intermediate energy range. It is also free from any approximation inherent in the TDCC method. The fact that the $e^+ + H$ scattering problem does not have exchange terms due to the distinguishability of the particles reduces the computational time. The goal of this paper is two fold: (1) to extend the TDH method to study the positron-hydrogen scattering system as one of the tests for its universal application and (2) to provide an independent check on the convergence of the TDCC method for the case of total angular momentum of zero ($L = 0$).

2 Theory

The time-dependent Schrödinger equation for positron-hydrogen scattering system has the form

$$H\Psi^{LM}(\mathbf{r}_1, \mathbf{r}_2, t) = \mathrm{i}\frac{\partial}{\partial t}\Psi^{LM}(\mathbf{r}_1, \mathbf{r}_2, t), \tag{1}$$

where $\Psi^{LM}(\mathbf{r}_1, \mathbf{r}_2, t)$ is the initial three-body wavefunction for the system for a fixed total angular momenta L, projection M and parity ϖ. The vectors $\mathbf{r}_1$ and $\mathbf{r}_2$ locate the electron and positron with respect to the assumed infinitely massive nucleus, which is fixed at the origin.

The non-relativistic Hamiltonian H of equation (1) for positron-hydrogen system (units in a.u.) takes the form of

$$H = -\frac{1}{2}\left(\nabla_1^2 + \nabla_2^2\right) + \frac{Zq_1}{r_1} + \frac{Zq_2}{r_2} + \frac{q_1 q_2}{|\mathbf{r}_1 - \mathbf{r}_2|}, \tag{2}$$

where Z (= 1) is the nuclear charge while q_1 (= −1) and q_2 (= 1) are the electron and positron charges, respectively.

The formal solution to equation (1) has the form of [23–28]

$$\Psi^{LM}(\mathbf{r}_1, \mathbf{r}_2, t + \Delta t) = \mathrm{e}^{-\mathrm{i}H\Delta t}\Psi^{LM}(\mathbf{r}_1, \mathbf{r}_2, t). \tag{3}$$

The evolution operator, $\mathrm{e}^{-\mathrm{i}H\Delta t}$ of equation (3) is evaluated using the Taylor series expansion, with maximum number of terms included to ensure its convergence. The initial wavefunction, $\Psi^{LM}(\mathbf{r}_1, \mathbf{r}_2, t = 0)$, can be expanded as [23–28]

$$\Psi_{\varpi}^{LM}(\mathbf{r}_1, \mathbf{r}_2, t = 0) = \frac{1}{r_1 r_2}\sum_{\ell_1=\varpi}^{L}\psi_{\ell_1}(r_1, r_2, \vartheta, t = 0)\mathcal{Y}_{\ell_1, L+\varpi-\ell_1}^{LM}(\hat{r}_1, \hat{r}_2). \tag{4}$$

The expansion coefficient ψ_{ℓ_1} is referred to as dynamical wavefunction. ℓ_1 is the angular momentum of the positron and ϖ is the parity ($\varpi = 0$ for this even parity case). The angular momentum of the electron, ℓ_2 is $(L + \varpi - \ell_1)$. The primary advantage of this approach lies in the fact that including ϑ in the expansion coefficient results in a small summation with $(L + 1)$ terms instead of an infinite over all possible (ℓ_1, ℓ_2) pairs. In fact, for the $L = 0$ with even parity, both the ℓ_1 and ℓ_2 are zero, therefore there is only one term in the expansion of equation (4).

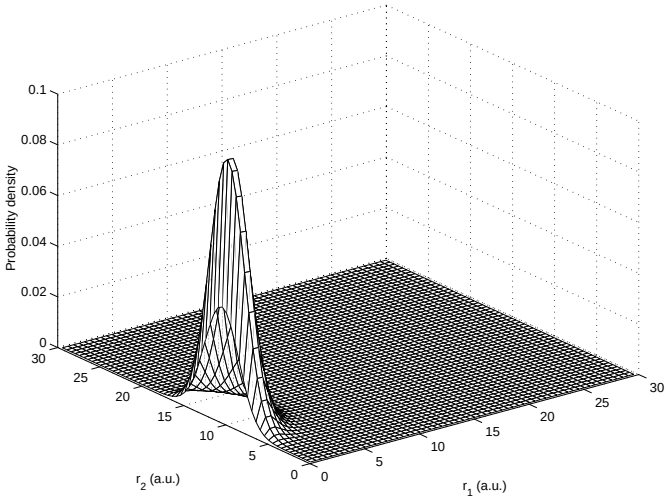

Fig. 1. Initial system wavefunction for energy of 30 eV with electron and positron at nearly zero degrees ($\vartheta = 4.1°$) from each other for $L = 0$. The positron is lying on the line passing through the center of the nucleus.

The initial dynamical wavefunction of equation (4) is formed from the product of the hydrogen atom ground state wavefunction and a positron projectile wavepacket. Let $\phi_{n\ell_2}(r)$ represent eigenstates of the hydrogen atom, n is the atomic energy level with ℓ_2 being the orbital angular momentum. Let $\chi_{\epsilon\ell_1}(r)$ be an incoming positron wavepacket with energy ϵ and angular momentum ℓ_1. The incoming positron wavepacket can be represented as

$$\chi_{\epsilon\ell_1}(r) = \frac{-\mathrm{i}kr}{(b^2\pi)^{\frac{1}{4}}}\mathrm{e}^{-\frac{(r-a)^2}{2b^2}}h_{\ell_1}^{-}(kr). \tag{5}$$

This wavepacket is composed of an incoming spherical Hankel function $h_{\ell_1}^{-}(kr)$ multiplied by a Gaussian shape function that localizes the wavepacket and defines its position, a and spatial spread, b. Since the ground state hydrogen atom wavefunction has $\ell_2 = m_2 = 0$, the angular momentum of the wavepacket will be equal to the total angular momenta for the system. For a system with zero total angular momentum, the dynamical wavefunction of equation (4) is expressed as [28]

$$\psi_{\ell_1}(r_1, r_2, \vartheta, t = 0) = \phi_{n0}(r_1)\chi_{\epsilon 0}(r_2). \tag{6}$$

Figure 1 shows the initial wavefunction plot of equation (4) for a projectile with energy of 30 eV, with the positron and electron being at near zero degrees ($\vartheta = 4.1°$) from each other. The wavepacket has a Gaussian width of 3.0 a.u. and centered at 10.0 a.u. along the r_2 direction. The hydrogen ground state wavefunction lies along the r_1 direction.

Table 1. Energies of the hydrogen atom bound states. Numerical energies were generated using basis spline collocation algorithm [31] with 60 grid points on a 30 a.u. grid size. The number in parenthesis is the power to base ten. The units are in a.u.

Bound states		Numerical		Analytical	% error
n	s	p	d	s	s
1	$-5.13(-1)$			$-5.00(-1)$	2.7(0)
2	$-1.26(-1)$	$-1.25(-1)$		$-1.25(-1)$	6.2(−1)
3	$-5.56(-2)$	$-5.56(-2)$	$-5.55(-2)$	$-5.60(-2)$	2.0(−2)

The probability that the electron is in the nlm bound state while the positron is in any possible state, P^{LM}_{nlm}, may be obtained by projecting the electron bound state onto the full wavefunction [29,30]

$$P^{LM}_{nlm}(t) = \int |\langle\langle \phi_{nlm}(\mathbf{r}_1)|\Psi^{LM}(\mathbf{r}_1,\mathbf{r}_2,t)\rangle\rangle|^2 \mathrm{d}\mathbf{r}_2, \qquad (7)$$

where $\phi_{nlm}(\mathbf{r}_1)$ describes a possible electron bound state of the atom, $\Psi^{LM}(\mathbf{r}_1,\mathbf{r}_2,t)$ is the time-dependent wavefunction for the two-particle system and the double bracket indicate integration over $\boldsymbol{r}_1$ only.

The time-dependent transfer probability is given by

$$P^{LM}_{\text{transfer}}(t) = 1 - \sum_{nlm} P^{LM}_{nlm}(t). \qquad (8)$$

The excitation cross-section is obtained from the asymptotic probability using [20]

$$\sigma^{LM}_{nl} = \frac{(2L+1)\pi}{k^2} \sum_m P^{LM}_{nlm}(t=T), \qquad (9)$$

where T is the final time, k is the wavepacket momentum and L is the total angular momentum, which is equal to zero in the present work. The transfer cross-section is calculated using [20]

$$\sigma^{LM}_{\text{transfer}} = \frac{(2L+1)\pi}{k^2} P^{LM}_{\text{transfer}}(t=T). \qquad (10)$$

3 Results

3.1 Numerical parameters

The numerical discretization of the wavefunctions and representation of operators were achieved using basis spline collocation algorithm [31]. To adequately discretize the initial wavefunction of equation (4) in the grid, the two numerical radial distances r_1 and r_2 were chosen to extend to 30 a.u. with 60 optimum grid points each while the maximum of angular component was 180° *i.e.* π radians with 12 grid points. The boundary conditions were set such that the wavefunction vanishes at the walls. With these requirements, the first grid point is located at $(0.25, 0.25, 4.1°)$ while the last one is at $(29.75, 29.75, 171.9°)$. 60 grid points produce essentially 60 pseudo energy levels (here after designated by n). Out of these 60, only the first three grid points produced reliable physical bound states as shown in Table 1. Thus, the excitations up to $n = 3$ hydrogen bound states are considered in this work. The $t = 0$ plot of Figure 1 shows the probable distance of the hydrogen atom $1s$ bound state as 1 a.u. along r_1 direction, which agrees with the analytical probable distance. At $t = 0$ a.u., the system wavefunction was set up such that there was no initial interaction between the positron and the atom.

3.2 Positron impact inelastic excitation probabilities

To illustrate the interaction processes within the intermediate energy range, a positron impact energy of 30 eV was chosen. This initial energy is well above the positronium-formation (6.8 eV) as well as above the ionization potential of hydrogen (13.6 eV). As time progresses, there will be three distinctive phases. In the first phase, there should be no interaction between the projectile and atom. Consequently, the two systems should be as far apart as practically possible. In this phase, the excitation probabilities should be zero.

The second phase is the interaction region. In this phase, the projectile wavepacket overlaps the atomic wavefunction and both wavefunctions become dramatically distorted. It is in this phase that the state of atom is expected to be changed as well as the state of the positron wavepacket. During this phase, many processes such as positron and nucleus excitations, multiple transitions and multiple decays could possibly take place. The excitation probabilities should be maximum.

The final phase is the post-interaction region where the projectile and the atom are separated. In this phase, the only changes that should be observed with increasing time is the motion and the spreading of the wavepacket for the continuum particles. Figure 2 shows the final wavefunction for the projectile energy of 30 eV with the positron and electron at near zero degrees ($\vartheta = 4.1°$) from each other. There are several possible consequences of the interaction process that can be inferred from this final phase. As the positron emerges out, it could leave the atom excited to one of many possible states or the atomic electron may gain enough energy from the positron to escape leaving the hydrogen atom ionized. The escaping electron could possibly combine with the positron to form positronium or may annihilate the positron to form a photon.

Figures 3 and 4 show $2s$, $2p$, $3s$, $3p$, and $3d$ time-dependent inelastic excitation probabilities at the

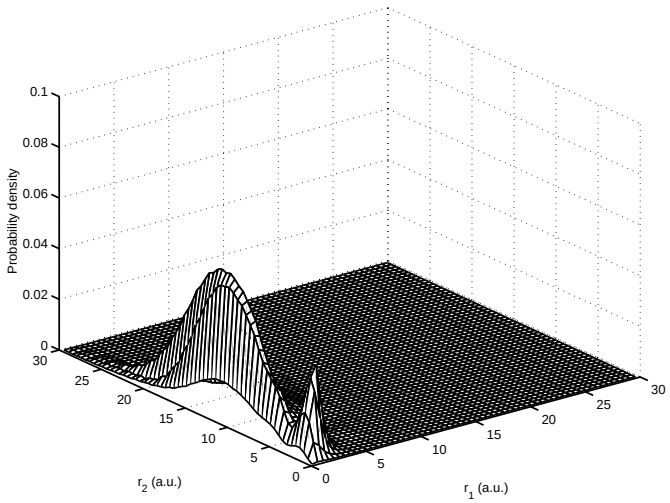

Fig. 2. Final system wavefunction for energy of 30 eV with electron and positron at nearly zero degrees ($\vartheta = 4.1^\circ$) from each other for $L = 0$. The positron is lying on the line passing through the center of the nucleus.

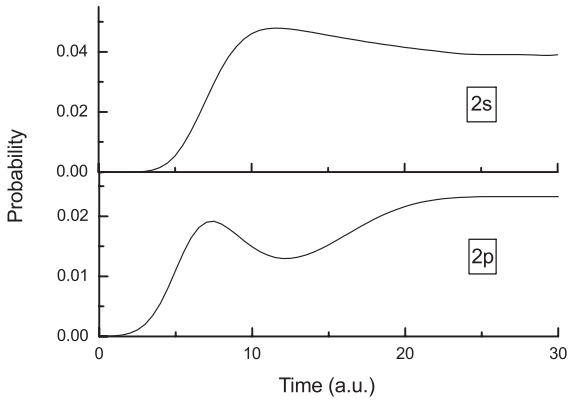

Fig. 3. Time-dependent probabilities for exciting the $n = 2$ states at 30 eV positron impact energy using the present TDH method for $L = 0$.

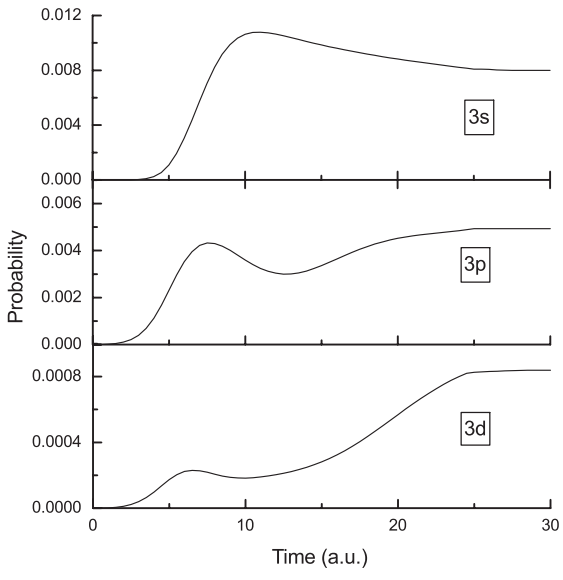

Fig. 4. Same as Figure 3 but for $n = 3$.

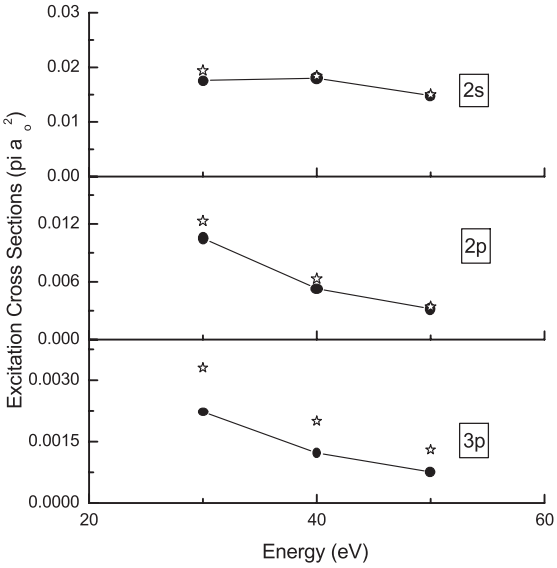

Fig. 5. Cross-sections for positron impact exciting $2s$, $2p$, and $3p$ atomic hydrogen states as a function of the incident positron energy for $L = 0$. The theoretical results are as follows: solid curve with dots at data points, present TDH results, stars, TDCC results (Ref. [20]).

intermediate positron impact energy of 30 eV. The probabilities are calculated from the time-dependent wavefunctions using equation (7). The excitation probabilities for the s states are zero between times of 0 and 2.5 a.u., then increase to maximum at about $t = 10$ a.u., there after remain stationary. For the p states, the probabilities start building up much earlier at $t = 1$ a.u., grow to maximum values then start falling off monotonically to about $t = 12$ a.u. leaving behind humps. The probabilities then re-build up again up to maxima at about $t = 20$ a.u. and remain flat for the rest of the time. The s states contribute more than twice the p states. The shapes of the curves in general represent the above described three phases in the collision process. The fact that the excitation probabilities have reached their asymptotic values indicates that the interaction process is over. The probability humps seen only with the p states could be due to the dipole allowed transitions associated with such states.

3.3 Positron impact excitation and transfer cross-sections

The time-dependent excitation cross-sections are calculated from the time-dependent asymptotic probabilities using equation (9). The cross-sections must be calculated when the projectile wavepacket is at a large distance from the interaction region as represented by Figure 2. In this final wavefunction (Fig. 2), the larger hump primarily contains all the excitation information while the flat region behind the hump contains ionization process. The smaller hump along the $r_1 = r_2$ contains the positronium information. Figure 5 shows the inelastic excitation cross-sections for the $2s$, $2p$ and $3p$ states at the positron impact energies

Table 2. Excitation cross-sections of hydrogen atom by positron at different intermediate impact energy range for $L = 0$. The units are in πa_0^2. The number in parenthesis is power to base 10.

	TDH			TDCC [20]		
Energy (eV)/nl state	$2s$	$2p$	$3p$	$2s$	$2p$	$3p$
30	1.76(−2)	1.05(−2)	2.23(−3)	1.94(−2)	1.23(−2)	3.30(−3)
40	1.80(−2)	5.30(−3)	1.22(−3)	1.84(−2)	6.30(−3)	2.00(−3)
50	1.48(−2)	3.18(−3)	7.61(−4)	1.50(−2)	3.40(−3)	1.30(−3)

Table 3. Transfer (combination of positronium and ionization) cross-sections for the positron-hydrogen scattering. The results are tabulated for the available typical energies from TDCC [30] calculations for $L = 0$. The cross-sections are in the units of πa_0^2. The results agree with each other to 3 decimal places.

Energy (eV)	TDH	TDCC [30]
30	0.0264	0.026
40	0.0350	0.035
50	0.0360	0.036

of 30, 40 and 50 eV for the system total angular momentum of zero ($L = 0$). The solid curve with circles at data points is the present TDH results. For comparison, the only other available theoretical calculations for the $L = 0$ TDCC [20] (stars) cross-sections are also displayed. Table 2 is the representative of the plotted values of the TDH and TDCC calculations. The TDH and TDCC $2s$ results are in better agreement than $2p$ and $3p$. The $3p$ results show the worst comparison. However, the agreement improves with the increase in energy for the presented excited states. In general, TDCC results are larger than the present TDH results. This trend of disagreement is not unique to the positron impact alone since it had also been observed in the case of the electron impact [27] where the disagreement was attributed to the non-convergence of the close coupling wavefunctions at lower energies. Since the present TDH method is free from any approximation and gave good agreement with the available results from other methods in the case of electron impact, it is possible to say that the TDCC results presented here had not converged. Admittedly, the excitation results presented here may not be adequate for a hard conclusion. For example, it would be interesting to see how the $3s$ and $3d$ results compare.

Table 3 shows the transfer cross-sections obtained from the present TDH and TDCC [30] approaches. The two calculations gave essentially exact results (to 3 decimal places) for all the representative energies. The transfer cross-sections represent the positronium and ionization cross-sections, which are not easy to separate from each other. Therefore, the excellent TDH and TDCC agreement may not give the insight on how the positronium or ionization cross-sections would compare but rather shows that the transfer cross-sections may be independent of the convergence of the number of coupled states.

4 Conclusion

The results from the time-dependent treatment of positron-hydrogen scattering has been presented for the total angular momentum of zero. It has been shown that the excitation states are accurately represented on the grid. The TDH excitation probabilities, which are used to calculate the excitation cross-sections have also been demonstrated to be asymptotic. However, these TDH excitation results have been shown not to be in good agreement in general with the available TDCC results. Unfortunately, there are no other similar theoretical results available to the author's knowledge for comparison. It would be interesting to see how the results from other non-close coupling methods compare. The presented transfer cross-sections are in excellent agreement, which indicate that there are adequate pseudostates in the numerical mesh for both the TDH and TDCC methods. Further work is in progress to attempt to separate the positronium and ionization cross-sections from the transfer cross-sections for this energy range.

The author acknowledges the generosity of Physics Department, University of Missouri-Rolla for providing the numerically intensive computational facilities for this work. The author would also like to thank Dr. D.R. Plante for providing the TDCC excitation cross-section results presented here.

References

1. R.W. Bussard, R. Ramaty, R.J. Drachman, Astophys. J. **228**, 928 (1979).
2. M. Leventhal, C.J. MacCallum, S.D. Barthelmy, N. Gehrels, B.J. Teegarden, J. Tueller, Nature **36**, 339 (1989).
3. F.M. Jacobsen, L.H. Andersen, B.I. Deutch, P. Hvelpind, H. Knudsen, M. Charlton, G. Larricchia, M. Holzscheiter, in: *Atomic Physics with Positrons*, edited by J.W. Humberston, E.A.G. Armour (plenum, New York, 1987), p. 333.
4. A.S. Ghosh, N.C. Sil, P. Madal, Phys. Rep. **87**, 313 (1982).
5. J.W. Humberston, Adv. At. Mol. Phys. **22**, 1 (1986).
6. H.R.J. Walters, A.A. Kernoghan, M.T. McAlinden, in *Proceedings of the XIX International Conference on the Physics of Electronic and Atomic Collisions*, AIP Conf. Proc. No. 360, edited by L.J. Dube, J.B.A. Mitchell, J.W. McConkey, C.E. Brion (AIP, Woodbury, 1995), p. 397.
7. M. Charlton, in *Photonic, electronic and atomic collisions*, edited by F. Aumayr, H. Winter (World Scientific, Singapore), pp. 361–371.

8. W. Raith, J. Phys. B **11**, 3081 (1978).
9. J.R. Winick, W.P. Reinhardt, Phys. Rev. A **18**, 910 (1978); *ibid.* **18**, 925 (1978).
10. K. Higgins, P.G. Burke, H.R.J. Walters, J. Phys. B **23**, 1345 (1990).
11. I. Bray, A.T. Stelbovics, Phys. Rev. A **49**, R2224 (1994).
12. K. Higgins, P.G. Burke, H.R.J. Walters, J. Phys. B **24**, L343 (1991).
13. K. Higgins, P.G. Burke, H.R.J. Walters, J. Phys. B **26**, 4269 (1993).
14. R.N. Hewitt, C.J. Noble, B.H. Bransden, J. Phys. B **24**, L635 (1991).
15. T.T. Gien, J. Phys. B **27**, L25 (1994).
16. J. Mitroy, A.T. Stelbovics, J. Phys. B **27**, L55 (1994).
17. A.A. Kernoghan, M.T. McAlinden, H.R.J. Walters, J. Phys. B **27**, L625 (1994).
18. M.T. McAlinden, A.A. Kernoghan, H.R.J. Walters, Hyperf. Interact. **89**, 161 (1994).
19. Y. Zhou, C.D. Lin, J. Phys. B **28**, L519 (1995).
20. D.R. Plante, M.S. Pindzola, Phys. Rev. A **57**, 1038 (1998).
21. J.B. Wang, N. Riste, S. Midgley, A.T. Stelbovics, J.F. Williams, Aust. J. Phys. **52**, 595 (1999).
22. E.A. Hylleraas, Z. Phys. **48**, 469 (1928).
23. C. Bottcher, J. Phys. B **14**, L349 (1981).
24. C. Bottcher, J. Phys. B. **15**, L463 (1982).
25. C. Bottcher, Adv. At. Mol. Phys. **20**, 241 (1985).
26. C. Bottcher, D.R. Schultz, D.H. Madison, Phys. Rev. A **49**, 1714 (1994).
27. G.D. Buffington, D.H. Madison, J.L. Peacher, D.R. Schultz, J. Phys. B: At. Mol. Opt. Phys. **32**, 2991 (1999).
28. D.O. Odero, J.L. Peacher, D.H. Madison, D.R. Schultz, Phys. Rev. A **63**, 022708 (2001).
29. W. Ihra, M. Draeger, G. Handke, H. Friedrich, Phys. Rev. A **52**, 3752 (1995).
30. M.S. Pindzola, D.R. Schultz, Phys. Rev. A **53**, 1525 (1996).
31. D.O. Odero, J.L. Peacher, D.H. Madison, Int. J. Mod. Phys. C **12**, 908 (2001).